Ligand Binding to Anti-Fluorescyl Antibodies: Stability of the Antigen Binding Site†

J. D. Müller and G. U. Nienhaus*

Department of Physics, University of Illinois at Urbana–Champaign, 1110 West Green Street, Urbana, Illinois 61801-3080

S. Y. Tetin and E. W. Voss

Department of Microbiology, University of Illinois at Urbana–Champaign, 407 South Goodwin Avenue, Urbana, Illinois 61801-3797

Received October 28, 1993; Revised Manuscript Received March 8, 1994®

ABSTRACT: The problem of protein stability is addressed with spectroscopic studies of equilibrium and kinetic properties of the binding of fluorescein to high-affinity monoclonal anti-fluorescyl antibodies (Mab 4-4-20), Fab fragments, and single-chain antibodies (SCA). SCA molecules contain only the variable domains of the antibody and an amino acid linker. The influence of glycerol on the antigen binding reaction is studied by circular dichroism, fluorescence, and absorption spectroscopy. The presence of glycerol in the solvent lowers the affinity of SCA for the ligand drastically, and the affinity even decreases toward lower temperatures. This effect is not observed in Fab and Mab. Analysis of the temperature jump kinetics shows that the dissociation reaction can be modeled as a two-state transition. The CD spectra indicate that the domain structure of the SCA remains unaltered in the presence of glycerol. Therefore, it is concluded that glycerol promotes the dissociation of the two variable domains of SCA. In Fab and Mab, the constant domains provide additional stabilization of the molecular structure at the antigen binding site.

The specific function of a protein molecule is often related to the presence of an active site. For many proteins, a much shorter amino acid sequence would suffice to establish an active site for a particular function, and the additional structural elements are believed to determine the overall stability and dynamic behavior of the molecule. Besides the protein structure itself, the surrounding solvent shell is of crucial importance for the stability and dynamic properties. Recently, the role of water in protein aggregation and protein reactions has found considerable attention (Rand, 1992; Colombo et al., 1992). A thorough understanding of the structural stabilization of proteins is very important, since it is a prerequisite for the *de novo* design of proteins with unique structure and function.

In contrast to active-site properties, the stabilizing interactions are mainly nonlocal and, therefore, more difficult to study. To approach the problem, one can examine how the function of the protein is modified when domains are removed that are distant from the active site. In a recent paper, Di Iorio et al. (1993) measured the flash photolysis recombination of carbon monoxide to mini-myoglobin (mini-Mb), a proteolytic fragment of horse heart Mb comprising residues 32–139. They noticed that structural fluctuations in this system are so large that they render the protein kinetically inefficient and structurally unstable.

For this paper, we addressed the problem of protein stability in a similar way. We performed ligand binding studies on the single-chain antibody SCA 4-4-20/212, a genetically engineered protein molecule derived from Mab 4-4-20, a high-affinity monoclonal antibody (IgG) specific for fluorescein (FL), for which an association coefficient $K_a \approx 2 \times 10^{10}$ M^{-1} has been reported at room temperature in aqueous solution (Kranz et al., 1982). The SCA contains only the variable light-chain (V_L) and heavy-chain (V_H) domains of the Mab 4-4-20 antibody, tethered by a 14 amino acid linker. Schematic drawings of the IgG molecule, the Fab, and the corresponding SCA are shown in Figure 1. The X-ray structure of the Fab fragments reveals that the fluorescein hapten is bound at the interface between the two variable domains (Herron et al., 1989). The interface is lined by a number of tyrosine and tryptophan residues that play a crucial role in binding the FL molecule, and they also contribute to the hydrophobic character of the interfacial surfaces. Although SCA 4-4-20 is a significantly modified protein molecule, its binding affinity toward the fluorescein ligand is only reduced by 4-fold compared with the whole Mab molecule at room temperature in pH 8.0 buffer (Bedzyk et al., 1990). This observation implies that under the given conditions, the two covalently linked variable domains simulate the antigen binding site of the parent antibody well in terms of structure and function.

Pervious experiments indicated that SCA 4-4-20 was considerably less thermally stable than the whole antibody (Tetin et al., 1992; Müller, 1992). We studied the influence of glycerol on both equilibrium and kinetic properties of fluorescein binding to Mab, Fab, and SCA as a function of temperature and solvent composition. SCA exhibits a marked loss of binding affinity in glycerol/water mixtures and at lower temperatures. The results indicate that the association of the two domains in SCA is weak and easily perturbed, leading to release of the antigen from the pocket. The pronounced destabilizing influence of glycerol on the binding affinity of SCA to fluorescein is surprising because glycerol is normally considered a cryoprotectant solvent that stabilizes the protein, as for example seen in the decrease of the cold denaturation temperature (Privalov, 1990). By contrast, no marked

† This work was supported in part by the National Science Foundation (Grant DMB 87-16476), Office of Naval Research (Grant N00014-92-J-1941), National Institutes of Health (Grants GM 18051 and RR 03155), and UIUC.

* Author to whom correspondence should be addressed.

® Abstract published in *Advance ACS Abstracts,* May 1, 1994.

0006-2960/94/0433-6221$04.50/0

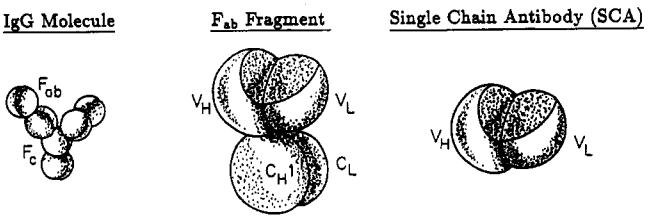

FIGURE 1: Schematic drawings of an IgG molecule, Fab fragment, and single-chain antibody (SCA). An IgG molecule consists of two identical light (L) and heavy (H) polypeptide chains covalently linked by disulfide bridges. The L chain folds into two domains, called V_L and C_L. The H chain contains four domains (V_H, C_{H1}, C_{H2}, and C_{H3}). A Fab fragment consists of a complete L chain linked by a disulfide bridge to a fragment of the H chain (V_H and C_{H1}). The variable domains (V_L and V_H) contain the active site of the antibody and can be linked by a short polypeptide chain to form a single-chain antibody (SCA). The linker is not shown.

destabilization was observed for Fab fragments or whole antibody molecules (Mab).

MATERIALS AND METHODS

Sample Preparation. Monoclonal anti-fluorescein antibodies (Mab) 4-4-20 (IgG2a,κ) were prepared from mouse ascites fluid by affinity purification (Kranz & Voss, 1981; Reinitz & Voss, 1984). Fab fragments were obtained by papain cleavage of Mab 4-4-20 and purified over a protein A–Sepharose 4B column (Weidner & Voss, 1991). SCA 4-4-20 protein was expressed in *Escherichia coli* and purified as described (Bird et al., 1988; Denzin et al., 1991). The protein samples were dissolved in 0.2 M potassium phosphate buffer at pH 8.0. All solutions were filtered through 0.22-μm Millipore low protein binding filters. For the glycerol/buffer mixtures, redistilled glycerol was added to the protein solutions.

Circular Dichroism. Protein samples were prepared in aqueous buffer and glycerol/buffer (75%/25%, v/v) solutions. Final concentrations of Mab 4-4-20 and SCA 4-4-20 were 1.3 and 4 μM, respectively. For CD measurements in the visible spectral range, fluorescein was added to the solutions to give a final FL concentration of 2.5 μM. CD experiments were performed on a CD 6 Dichrograph spectrometer (Jobin-Yvon/SPEX). The samples were kept at room temperature in the N_2-purged sample chamber in quartz cuvettes, and CD spectra were taken in the UV region between 200 and 250 nm and in the visible region between 420 and 560 nm. In both regions, the spectral resolution was 2 nm.

Fluorescence. Fluorescence intensity measurements were performed using a photon counting spectrofluorometer (Gregg-PC, ISS Instruments, Champaign, IL). The samples were illuminated with light from a xenon lamp passed through a monochromator at 470 nm with a width of 8 nm (full width at half-maximum). At the light levels used here, bleaching of the fluorescence is insignificant (Seybold et al., 1969). Emission spectra were recorded in the wavelength region between 500 and 640 nm. The sample temperature was controlled by circulating a methanol/water mixture from a thermostatic bath. Efficient quenching of fluorescein fluorescence on binding to Mab and Fab 4-4-20 (Swindlehurst & Voss, 1991) was used to determine the binding affinities in solutions containing glycerol and phosphate buffer (60%/40%, v/v) at different temperatures. For the experiments, a series of 15 protein solutions was obtained by successive dilution of the protein stock solution by a factor of 2. To 1 mL of protein solution were added 3 mL of glycerol and 1 mL of fluorescein solution (70 nM). Integrated fluorescence intensity from each of the samples was measured. The fluorescence intensity was plotted against the logarithm of the protein concentration, and the association coefficient, K_a, was determined at the midpoint of the curve.

Visible Spectroscopy, Temperature-Jump Experiments. For absorption spectroscopy, glycerol/buffer solutions (60%/40%, v/v) of SCA 4-4-20 (13 μM) with FL (10 μM), Fab 4-4-20 (15 μM) with FL (10 μM), and FL (10 μM) only were prepared. Furthermore, a very dilute sample of Fab 4-4-20 (450 nM) and FL (560 nM) was prepared to estimate the affinity of Fab fragments. FL absorbs in the visible with λ_{max} = 490 nm in aqueous solutions and 493 nm in glycerol/water mixtures; upon binding to the antibody, a bathochromic shift to 506 nm is observed. Use was made of this spectral change to monitor the antigen binding reaction.

The samples were loaded into lucite cuvettes with 10-mm path length that were kept inside a block of oxygen-free high-conductivity copper mounted on the cold-finger of a closed-cycle helium refrigerator (Model 22C, CTI Cryogenics, Waltham, MA). The temperature was measured with a silicone temperature sensor diode and regulated with a digital temperature controller (Model DRC93C, Lake Shore Cryotronics, Westerville, OH). The cryogenic setup was mounted on a Cary-14 spectrophotometer interfaced to an IBM PC/AT (On-Line Instrument Systems Inc., Jefferson, GA). The wavelength accuracy and reproducibility are 0.2 nm and 0.05 nm, respectively. Typically, spectra were taken between 400 and 600 nm, with 1-nm resolution. The time for a single scan was 100 s.

Temperature-jump experiments were performed by first equilibrating the sample at a particular temperature, T_0. Then, the temperature was changed to the new temperature T within 10–100 s, dependent on the temperature interval. The relaxation was monitored over a time span of up to a few days by measuring at a fixed wavelength, λ = 509 nm, or, for the slower relaxations, by taking entire absorption spectra. The two methods led to identical results. The T-jump was performed from the temperature T_0 = 280 K, where equilibrium is reached in less than an hour, to lower temperatures between 230 and 265 K.

Analysis of Kinetic Data. We used the singular value decomposition (SVD) algorithm (Press et al., 1989) to analyze the observed spectral changes in terms of a linear combination of a few spectra characteristic of the different species that contribute significantly to the observed kinetics. From the T-jump experiments, a series of spectra were obtained as a function of time, t. The spectra can be represented by an $m \times n$ matrix, $\mathbf{A}(\lambda,t)$, where the indices m and n denote the wavelengths λ_m and times t_n. This matrix is highly singular when the time evolution of the total spectrum can be described by linear combination of a few spectra with time-dependent coefficients. According to the SVD algorithm, the matrix $\mathbf{A}(\lambda,t)$ can be written as a product of three matrices:

$$\mathbf{A}(\lambda,t) = \mathbf{USV}^{\mathrm{T}} \quad (1)$$

$\mathbf{U}$ is an $m \times n$ matrix with orthonormal columns that form a complete basis set of spectra, so that $\mathbf{A}(\lambda,t)$ can be described as a linear combination of these basis spectra at any time. The $n \times n$ diagonal matrix $\mathbf{S}$ contains the singular values s_{ii}, which represent a time-independent weighting factor for the different basis spectra. The matrix $\mathbf{V}^{\mathrm{T}}$ is the transpose of an $n \times n$ matrix containing orthonormal rows and columns. $\mathbf{V}^{\mathrm{T}}$ contains sets of coefficients for each basis spectrum that represent its time dependence. The SVD analysis is a very efficient data reduction algorithm when only a few basis spectra contribute to the spectrum: It reduces the number of data that describe the kinetics from $m \times n$ to the number of significant basis

spectra times $m + n + 1$. The significance of a basis spectrum can be judged from its singular value s_{ii} and the autocorrelation of its time dependence. The orthonormal basis spectra that are obtained from the SVD have no *a priori* physical meaning, but they can be used to generate physical spectra as linear combinations.

As shown below, the SVD analysis revealed that all spectral changes can be described using two basis spectra. This observation justifies monitoring the extent of the reaction directly from absorbance measurements at a fixed wavelength, $\lambda = 509$ nm. When collecting entire spectra, we obtained the kinetics by SVD analysis of the difference spectrum $\Delta\mathbf{A}(\lambda,t) = \mathbf{A}(\lambda,t) - \mathbf{A}(\lambda,\infty)$. Since the concentrations of protein and ligand are of the same order of magnitude, the kinetics are not pseudo first order, but follow a bimolecular rate law. The time dependence of the FL concentration, $C_{FL}(t)$, is then given by

$$C_{FL}(t) = C_{FL}(\infty) + \left[\left(\frac{x}{\Delta C_{FL}} + 1\right) exp(xk_a t) - 1\right]^{-1} \quad (2)$$

with $\Delta C_{FL} = C_{FL}(0) - C_{FL}(\infty)$ and $x = [(C^{tot}_{SCA} - C^{tot}_{FL} + K_a^{-1})^2 + 4K_a^{-1}C^{tot}_{FL}]^{1/2}$, where C^{tot}_{SCA} and C^{tot}_{FL} are the total concentrations of SCA and FL, respectively, and K_a is the equilibrium association coefficient, which can easily be determined by decomposition of the spectrum into that of free FL in solution plus that of FL bound to the antibody. The association rate coefficient is denoted by k_a. We performed nonlinear least-squares fits of the bimolecular rate expression to extract the association and dissociation rate coefficients.

RESULTS AND DISCUSSION

CD Studies of Solvent Effects. Free fluorescein in solution does not exhibit circular dichroism, but acquires it upon binding to antibodies (Gollogly & Cathou, 1974; Voss & Watt, 1977; Tetin et al., 1992). In Figure 2a, we compare the CD spectra of FL bound to Mab and SCA 4-4-20 in aqueous buffer and in glycerol/buffer (75%/25%, v/v) mixtures at room temperature. The data are given in terms of molar ellipticites, $[\theta]$, of the bound fluorescein hapten. The CD spectra of FL bound to both Mab and SCA, measured in buffer, track the absorbance spectra of FL. They exhibit maxima at 506 nm. For fluorescein bound to Mab 4-4-20 in the glycerol solvent (Figure 2a), a small red-shift by 2 nm is observed in the CD spectrum. For free fluorescein, the absorbance spectrum is red-shifted by 5 nm in the glycerol/buffer solvent compared with buffer only, owing to the different dielectric properties. The smaller shift on binding to the antibody suggests mainly screening of the chromophore by the protein and not so much structural changes of the protein in response to the different solvents. The CD spectrum of FL bound to SCA 4-4-20 in aqueous solution is identical to the Mab spectrum. However, in the glycerol/buffer mixture, the CD signal has almost vanished. The area under the small peak around 510 nm indicates that, on the average, only about 4% of fluorescein is still bound. The resulting association coefficient, K_a, in 75% glycerol solvent is $\approx 10^4$ M^{-1}, more than 6 orders of magnitude below the value reported for aqueous solvent.

Figure 2b shows UV spectra of the same samples, but without fluorescein. Here, the spectral amplitudes are normalized to give the molar mean-residue-weight ellipticities, $[\theta]_{MWR}$. While the Mab samples exhibit only weak shoulders at 230 nm, both SCA samples show pronounced minima. SCA has a much higher relative content of tyrosine and tryptophan residues; therefore, this minimum has been attributed to the aromatic side chains (Tetin et al., 1992). This view is supported

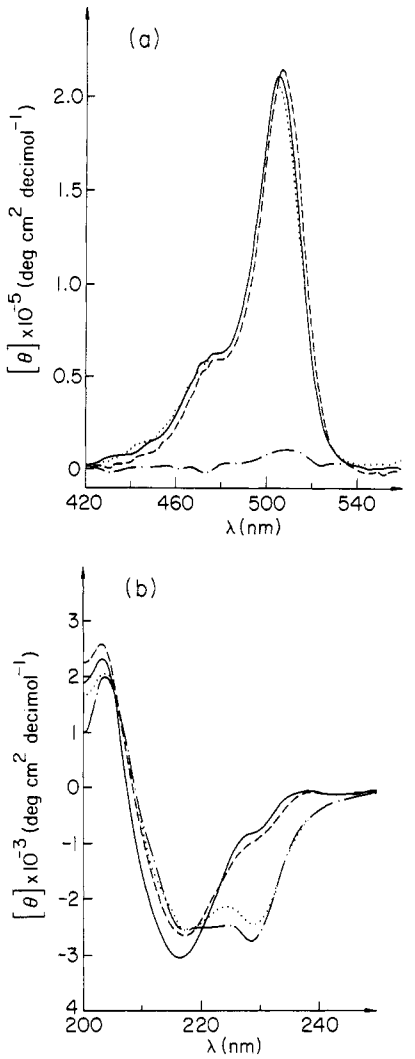

FIGURE 2: CD spectra of (a) fluorescein/antibody solutions, measured between 420 and 560 nm, and (b) antibody solutions without fluorescein, measured between 200 and 250 nm. As antibody samples, Mab 4-4-20 in buffer solution (solid line) and in glycerol/buffer (75%/25%, v/v) (dashed line) was used, and SCA 4-4-20 in buffer solution (dotted line) and in glycerol/buffer (75%/25%, v/v) (dashed–dotted line) was used.

in theoretical calculations by Woody (1978, 1987). Between 200 and 220 nm, all four spectra are very similar, with maxima at 205 nm and minima at 217 nm. These spectral features are typical for proteins with β-sheets as the main folding motif (Saxena & Wetlaufer, 1971). The pronounced affinity difference observed for SCA 4-4-20 in the two solvents is not reflected in the UV CD spectra. We conclude that the secondary structure of the two variable domains is not significantly altered by addition of glycerol to the solvent. The interface between the two variable domains is lined with apolar amino acid residues; therefore, their association is driven by hydrophobic forces. Addition of glycerol makes the solvent less polar, and the domain–domain interactions are weakened or disrupted. Since the fluorescein antigen is bound in the interface between the two variable domains, the binding affinity decreases in less polar solvents.

Temperature Dependence of Binding Affinities. To determine the affinity coefficient, K_a, for Mab 4-4-20 and SCA 4-4-20, we used fluorescence and absorption spectroscopies. The affinity of FL to SCA in glycerol/water mixtures decreases with increasing concentration of glycerol. For the experiments, a mixture of 60% glycerol and 40% buffer (v/v) was chosen to obtain affinities convenient for the experimental procedures.

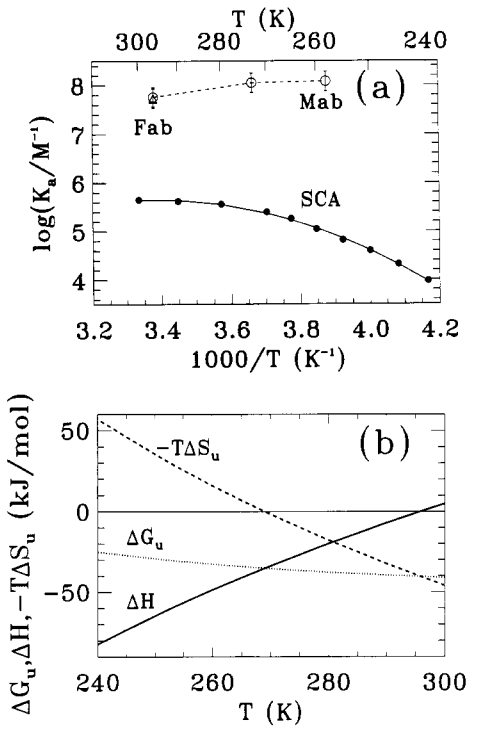

FIGURE 3: (a) van't Hoff plot of equilibrium coefficients, K_a of fluorescein binding to Fab 4-4-20 (triangle), Mab 4-4-20 (open circles), and SCA 4-4-20 (filled circles) in glycerol/buffer (60%/40%, v/v). The dashed line is drawn to guide the eye, the solid line is a fit of a parabola to the experimental data. (b) Thermodynamic parameters for the ligand binding reaction. Dotted line, unitary free energy difference ΔG_u; solid line, enthalpy difference ΔH; dashed line, entropic part of ΔG_u, $-T\Delta S_u$.

The affinity coefficient, K_a, for fluorescein binding to monoclonal antibodies Mab 4-4-20 and Fab fragments was measured using fluorescence techniques. Figure 3 shows the data for three different temperatures, 258, 273, and 297 K, in a van't Hoff plot. The association coefficients close to 10^8 M^{-1} are 300-fold lower than those reported for aqueous solutions. Considering the error bars, it is safe to say that they depend only weakly on temperature. A similar decrease in binding affinity was observed for Fab 4-4-20 crystals with 40% MPD (2-methyl-2,4-pentanediol) added to the crystallization solutions (Gibson et al., 1988), where the effect has been attributed predominantly to conformational changes of the protein in the more hydrophobic solvent, consistent with the observation that the temperature for heat denaturation was significantly decreased.

Absorption spectroscopy of fluorescein in the visible region was used to measure the spectra of free FL and the FL–Fab 4-4-20 complex in the temperature range 230–300 K. At high concentrations of Fab (15 μM) and FL (10 μM), practically all FL molecules are bound to the antibodies between 230 and 300 K. Using a very dilute Fab/FL sample (450/560 nM), we were able to generate 28% ligand-free binding sites, independent of temperature between 230 and 300 K, corresponding to an affinity coefficient $K_a = 10^{7.8\pm0.4}$ M^{-1}. After the samples were cooled, no time-dependent changes of the spectra were observed on the time scale of days, indicating that the samples were in equilibrium. Similar results were obtained when using Mab instead of Fab fragments.

Absorption spectroscopy of fluorescein in the visible was also employed to determine K_a for the single-chain antibodies in glycerol/buffer (60%/40%, v/v). By contrast with the Fab samples, the absorption spectrum of SCA 4-4-20 with

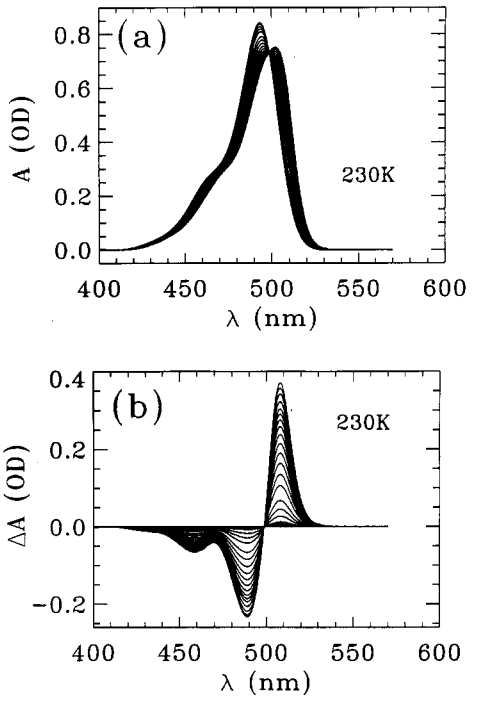

FIGURE 4: Time dependence of (a) the absorbance spectrum and (b) the absorbance difference spectrum of a sample containing SCA 4-4-20 and fluorescein in glycerol/buffer (60%/40%, v/v) after a temperature jump from 280 to 230 K. The difference spectra were calculated with respect to the last spectrum in the time series.

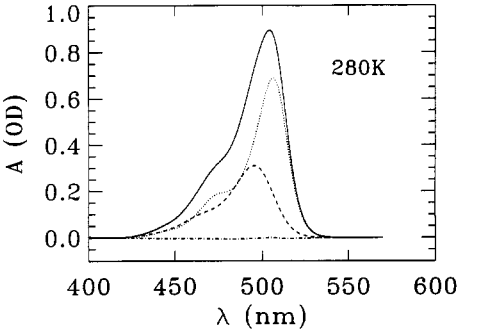

FIGURE 5: Superposition of the spectra of free fluorescein (dashed line) and fluorescein bound to Fab 4-4-20 (dotted line) to give the spectrum of a glycerol/buffer solution of SCA 4-4-20 with FL at 280 K (solid line). The dashed–dotted line represents the residuals. The spectra indicate that 69% of the FL is bound to SCA 4-4-20.

fluorescein evolves slowly with time after changing the sample temperature. Figure 4a shows the temporal evolution of the spectrum after a T-jump from 280 to 230 K. The peak wavelength λ_{max} shifts from 502 to 493 nm. The existence of an isosbestic point at 498 nm and the time-invariant shape of the difference spectrum in Figure 4b suggest that the spectral changes reflect a transition between two species. Indeed, the SVD analysis verified that two basis spectra are sufficient to describe the entire set of data. After relaxation of the SCA/FL system at 230 K, the spectrum is that of free fluorescein in solution. Furthermore, the spectra of the SCA 4-4-20 sample with FL can be superimposed from the spectra of FL-ligated Fab 4-4-20 and free FL in solution at all times and temperatures, as shown in Figure 5 for 280 K. Therefore, the spectra of FL bound to Fab and SCA are identical, and the spectral changes on cooling indicate the release of the FL ligand from SCA 4-4-20.

Spectra taken upon complete relaxation of the protein/ligand system after changing the temperature were decomposed using SVD. The temperature dependence of the

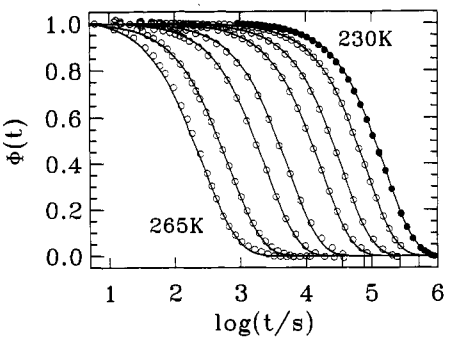

FIGURE 6: Relaxation functions for the temperature-jump kinetics of SCA 4-4-20 and FL in glycerol/buffer (60%/40%, v/v). Starting from 280 K, the temperature was lowered to temperatures between 230 and 265 K (steps of 5 K). The kinetics were measured by following the absorbance at 509 nm (open circles) except for 230 K, where they were obtained from the SVD analysis of absorption difference spectra (closed circles). The lines are least-squares fits of the bimolecular rate law (eq 2) to the experimental data.

equilibrium association coefficient, K_a, of the SCA/FL system is shown in the van't Hoff plot (Figure 3a) together with the Mab and Fab data. In the van't Hoff plot, the temperature dependence can be described with a parabola within experimental error (solid line in Figure 3a), but the data may also be approximated as linear between 240 and 270 K. Figure 3b shows the differences in the unitary free energy, ΔG_u, enthalpy ΔH, and the entropic part of ΔG_u, $-T\Delta S_u$, between the ligand-bound and unbound forms that result from the temperature dependence of K_a. ΔH and $-T\Delta S_u$ are strongly temperature-dependent. The entropic contribution changes sign at 268 K and becomes destabilizing below that temperature. The temperature dependencies of both enthalpy and entropy compensate each other to a large extent, so that ΔG_u is comparatively weakly temperature-dependent.

Similar binding affinities of SCA and Mab/Fab in aqueous buffer at room temperature imply that the antigen binding sites are functionally very similar. When using glycerol/buffer mixtures, the fluorescein binding affinities of Mab and Fab are more than 2 decades larger than that of single-chain antibodies at 300 K. While Mab and Fab do not show a pronounced temperature effect, the FL binding affinity of SCA decreases markedly with temperature. Evidently, the affinity decrease and the temperature effect are not intrinsic to the ligand binding reaction, but reflect structural changes of the SCA.

Antigen–Antibody Binding Kinetics. Kinetic data from T-jump experiments are plotted in Figure 6 as normalized relaxation functions:

$$\Phi(t) = \frac{M(t) - M(\infty)}{M(0) - M(\infty)} \qquad (3)$$

For the data in Figure 6, the observable M was the absorbance at 509 nm, except for the measurement at 230 K, where we used the SVD amplitude of the difference spectrum. The solid lines represent fits of the bimolecular rate law, eq 2, to the experimental data. The good agreement of theory and data indicates that the reaction is well modeled as a bimolecular reaction with two unique rate coefficients: the second-order association rate coefficient, k_a, and the first-order dissociation rate coefficient, k_d. Their temperature dependencies are given in an Arrhenius plot in Figure 7. In the narrow temperature interval between 230 and 265 K, the data can be modeled with the Arrhenius law. For the association reaction, we obtain a preexponential $A_a^\ddagger = 10^{31.4}$ s^{-1} M^{-1} and an activation enthalpy $H_a^\ddagger = 148$ kJ/mol. For the dissociation reaction, the

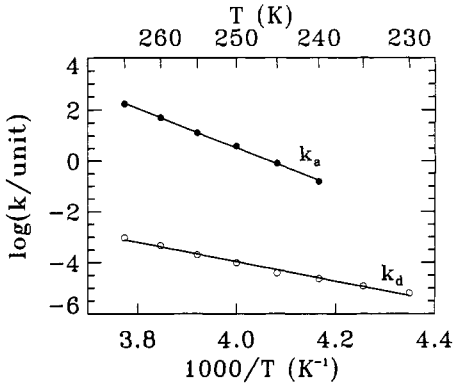

FIGURE 7: Arrhenius plot of the association and dissociation rate coefficients k_a (in M^{-1} s^{-1}) and k_d (in s^{-1}). The rate coefficients were determined by least-squares fits to the data shown in Figure 6.

Arrhenius parameters are $A_d^\ddagger = 10^{11.3}$ s^{-1} and $H_d^\ddagger = 71$ kJ/mol. The rate processes cannot be understood with transition-state theory, as indicated by the unphysically large parameters of the association reaction. Furthermore, Arrhenius extrapolation of k_a and k_d toward higher temperatures would not be consistent with the saturation behavior of K_a (Figure 3). Therefore, the Arrhenius parameters serve as a mere parameterization of the kinetics. Other relations, borrowed from the physics of viscous liquids and polymers, have been used to describe rate processes in proteins over wide temperature ranges (Steinbach et al., 1991).

The observed large activation enthalpies are typical for rate processes involving proteins in viscous liquids. In biomolecular reactions, solvent viscosity is crucially involved in the kinetics in two ways: (i) The viscous solvent may limit the bimolecular reaction rate by suppressing the number of possible encounters per unit time (diffusion control). (ii) The kinetics of the biomolecular reaction itself may depend on the solvent viscosity (Kramers, 1940; Frauenfelder & Wolynes, 1985). For example, protein reactions may be accompanied by conformational transitions, which are viscosity dependent owing to the strong interaction between biomolecule and solvent shell (Beece et al., 1980; Frauenfelder, 1985; Young et al., 1991; Ansari et al., 1992; Kovacs et al., 1993). We have found activation enthalpies similar to $H_d^\ddagger$ of the SCA/FL system for the cis/trans isomerization of bacteriorhodopsin (86 kJ/mol) (Kovacs et al., 1993) and for the $A_0 \rightleftharpoons A_1$ transition in myoglobin (74 kJ/mol) (Young et al., 1991) in glycerol/water mixtures. The kinetic processes in bacteriorhodopsin and myoglobin are entirely conformational transitions, whereas in SCA/FL, there is the ligand dissociation reaction in addition to protein motions. Thermodynamic studies of anti-fluorescein antibodies have shown that ligand binding enthalpies are small and tend to decrease with temperature (Herron, 1986). Therefore, ligand binding will not govern domain aggregation, but will certainly assist in stabilization of the two variable domains. The considerably higher barrier $H_a^\ddagger$ for ligand association is expected, since it not only involves conformational motion but also involves the bimolecular encounter, which is influenced by strongly temperature-dependent diffusivities. If we assume a conformational activation enthalpy similar to $H_d^\ddagger$ and neglect the ligand binding barrier, we obtain an apparent barrier for the bimolecular association of 77 kJ/mol. Values around 70 kJ/mol are observed in the bimolecular binding of diatomic ligands to proteins at low temperatures in glycerol/water mixtures (Steinbach et al., 1991; Ehrenstein & Nienhaus, 1992). Therefore, a substantial activation enthalpy for fluorescein binding appears unlikely.

CONCLUSIONS

Hydrophobic, vibrational, and conformational effects are important thermodynamic driving forces in many biochemical reactions (Sturtevant, 1977). Since fluorescein is an aromatic molecule, and the binding pocket is lined by aromatic, apolar residues, the hydrophobic effect is relevant in the binding of FL to anti-fluorescein antibodies. Antigen binding can also lead to ligand-induced changes of the vibrational spectrum of the protein. Sturtevant (1977) attributed the low entropy changes in protein reactions to this effect. We believe that the effects of ligand binding on both equilibria and fluctuations between conformational substrates are even more important in the context of antigen–antibody interactions. The variable domains are extremely flexible, which may be functionally important to accommodate slightly different antigenic structures. In many cases, the immunoglobulin molecule changes its structure upon antigen binding, and conformational fluctuations in the active site are expected to be reduced as a consequence of additional bonds and steric constraints provided by the antigen (Kranz et al., 1982; Herron et al., 1986). This view is supported by the fact that antibodies crystallize preferably in the antigen-bound state.

The affinity of anti-fluorescein antibodies decreases markedly when glycerol is added to the aqueous buffer solution. The hydrophobic effect on the ligand binding reaction can be invoked to explain the affinity reduction. However, from thermodynamic studies, Gibson et al. (1988) concluded that conformational changes are more important. This view is supported by the difference in the association coefficient K_a between Mab and SCA (Figure 3). While Fab and Mab retain high affinity for the FL ligand in the presence of glycerol, SCA drastically loses affinity. The different behavior of SCA implies that glycerol does not affect the affinity through interference with the antigen binding site; it rather suggests domain dissociation of the SCA as the structural mechanism. The identical behavior of Mab and Fab indicates that the two constant domains adjacent to the variable domains have a stabilizing effect on the antigen binding site. They assist in the association of the variable domains by providing additional bonds, and they may also dampen excessive fluctuations. The 2 orders of magnitude higher binding affinities of Fab and Mab compared with SCA at 300 K suggest that the constant domains contribute to the ligand binding free energy with about 12 kJ/mol at 300 K. In single-chain antibodies, the domain association is weak, and diminished hydrophobic interactions make it more favorable to expose apolar groups to the solvent (Brandts & Hunt, 1967; Velicelebi & Sturtevant, 1979), with concomitant destabilization or complete destruction of the antigen binding site. The decrease in the affinity of SCA 4-4-20 (Figure 3) is the typical signature of a cold denaturation effect (Privalov, 1990), which leads to a lowering of the enthalpy and entropy of the protein/solvent system. The "molten globule" state has been introduced to characterize a compact, denatured protein molecule with still intact secondary structure but severely disrupted connections on the tertiary level (Dolgikh et al., 1981; Ohgushi & Wada, 1983). The CD spectra in Figure 2 show that the domain structure is unchanged in SCA in glycerol/water solution, whereas the low affinity indicates severe structural changes at the domain interface. The fact that Fab and Mab samples do not exhibit a decrease of affinity with temperature leads us to believe that the two variable domains remain in their native structures under the experimental conditions employed and that the decrease in ligand binding affinity in more hydrophobic solvents is caused by structural changes that are localized at the domain–domain interface.

ACKNOWLEDGMENT

It is a great pleasure to acknowledge all members of the Biological Physics Group for their collaboration. Special thanks to Professor Hans Frauenfelder for valuable comments on the manuscript. Fluorescence and CD experiments were performed at the Laboratory for Fluorescence Dynamics (LFD) at the University of Illinois at Urbana–Champaign.

REFERENCES

Ansari, A., Jones, C. M., Henry, E. R., Hofrichter, J., & Eaton, W. A. (1992) *Science (Washington, D.C.) 256*, 1796–1798.
Bedzyk, W. D., Weidner, K., Denzin, L. K., Johnson, L. S., Hardman, K. D., Pantoliano, M. W., Asel, E. D., & Voss, E. W., Jr. (1990) *J. Biol. Chem. 265*, 18615–18620.
Beece, D., Eisenstein, L., Frauenfelder, H., Good, D., Marden, M. C., Reinisch, L., Reynolds, A. H., Sorensen, L. B., & Yue, K. T. (1980) *Biochemistry 19*, 5147–5157.
Bird, R. E., Hardman, K. D., Jacobson, J. W., Johnson, S., Kaufman, B. M., Lee, S. M., Pope, S. H., Riordan, G. S., & Whitlow, M. (1988) *Science 242*, 423–426.
Brandts, J. F., & Hunt, L. (1967) *J. Am. Chem. Soc. 89*, 4826–4838.
Colombo, M. F., Rau, D. C., & Parsegian, V. A. (1992) *Science 256*, 655–659.
Denzin, L. K., Whitlow, M., & Voss, E. W., Jr. (1991) *J. Biol. Chem. 266*, 14095–14103.
Di Iorio, E. E., Yu, W., Calonder, C., Winterhalter, K. H., De Sanctis, G., Falcioni, G., Ascoli, F., Giardina, B., & Brunori, M. (1993) *Proc. Natl. Acad. Sci. U.S.A. 90*, 2025–2029.
Dolgikh, D. A., Gilmanshin, R. I., Brazhnikov, E. V., Bychkova, V. E., Semisotnov, G. V., Venyaminov, S. Yu., & Ptytsin, O. B. (1981) *FEBS Lett. 136*, 311–315.
Ehrenstein, D., & Nienhaus, G. U. (1992) *Proc. Natl. Acad. Sci. U.S.A. 89*, 9681–9685.
Frauenfelder, H., & Wolynes, P. G. (1985) *Science 229*, 337–345.
Gibson, A. L., Herron, J. L., He, X.-M., Patrick, V. A., Mason, M. L., Lin, J.-N., Kranz, D. N., Voss, E. W., Jr., & Edmundson, A. B. (1988) *Proteins: Struct., Funct., Genet. 3*, 155–160.
Gollogly, J. R., & Cathou, R. E. (1974) *J. Immunol. 113*, 1457–1467.
Herron, J. N., Kranz, D. M., Jameson, D. M., & Voss, E. W., Jr. (1986) *Biochemistry 25*, 4602–4609.
Herron, J. N., He, X., Mason, M. L., Voss, E. W., Jr., & Edmundson, A. B. (1989) *Proteins: Struct., Funct., Genet. 5*, 271–280.
Kovacs, I., Nienhaus, G. U., Philipp, R., & Xie, A. (1993) *Biophys. J. 64*, 1187–1193.
Kramers, H. A. (1940) *Physica 7*, 284–304.
Kranz, D. M., & Voss, E. W., Jr. (1981) *Mol. Immunol. 18*, 889–898.
Kranz, D. M., Herron, J. N., & Voss, E. W., Jr. (1982) *J. Biol. Chem. 257*, 6987–6995.
Müller, J. D. (1992) Diploma Thesis, TU München.
Ohgushi, M., & Wada, A. (1983) *FEBS Lett. 164*, 21–24.
Press, W. H., Flannery, S. A., Teukolsky, S. A., & Vetterling, W. T. (1989) *Numerical Recipes in C*, Cambridge University Press, Cambridge, U.K.
Privalov, P. (1990) *Crit. Rev. Biochem. Mol. Biol. 25*, 281–305.
Rand, R. P. (1992) *Science 256*, 618.
Reinitz, D. M., & Voss, E. W., Jr. (1984) *Mol. Immunol. 21*, 775–784.
Saxena, V. P., & Wetlaufer, D. B. (1971) *Proc. Natl. Acad. Sci. U.S.A. 68*, 969–973.

Seybold, P. G., Gouterman, M., & Callis, J. (1969) *Photochem. Photobiol. 9*, 229–242.

Steinbach, P. J., Ansari, A., Berendzen, J., Braunstein, D., Chu, K., Cowen, B. R., Ehrenstein, D., Frauenfelder, H., Johnson, J. B., Lamb, D. C., Luck, S., Mourant, J. R., Nienhaus, G. U., Ormos, P., Philipp, R., Xie, A., & Young, R. D. (1991) *Biochemistry 30*, 3988–4001.

Sturtevant, J. M. (1977) *Proc. Natl. Acad. Sci. U.S.A. 74*, 2236–2240.

Swindlehurst, C. A., & Voss, E. W., Jr. (1991) *Biophys. J. 59*, 619–628.

Tetin, S. Yu., Mantulin, W. W., Denzin, L. K., Weidner, K. M., & Voss, E. W., Jr. (1992) *Biochemistry 31*, 12029–12034.

Velicelebi, G., & Sturtevant, J. M. (1979) *Biochemistry 18*, 1180–1186.

Voss, E. W., Jr., & Watt, R. M. (1977) *Immunochemistry 14*, 237–241.

Weidner, K. M., & Voss, E. W., Jr. (1991) *J. Biol. Chem. 266*, 2513–2519.

Woody, R. W. (1978) *Biopolymers 17*, 1451–1467.

Woody, R. W. (1987) in *Proceedings of the Federation of European Chemical Societies Second International Conference on Circular Dichroism* (Kajtar, M., Ed.) pp 38–56, VCH Publishers, New York.

Young, R. D., Frauenfelder, H., Johnson, J. B., Lamb, D. C., Nienhaus, G. U., Philipp, R., & Scholl, R. (1991) *Chem. Phys. 158*, 315–327.